

# 6-Gingerol, a Bioactive Compound of *Zingiber officinale*, Ameliorates High-Fat High-Fructose Diet-Induced Non-Alcoholic Related Fatty Liver Disease in Rats

Shirly Gunawan<sup>1</sup>, Vivian Soetikno<sup>2</sup>, Erni Hernawati Purwaningsih<sup>3</sup>, Frans Ferdinal<sup>4</sup>, Puspita Eka Wuyung<sup>5,6</sup>, Dwi Ramadhani<sup>7</sup>

<sup>1</sup>Department of Pharmacology, Faculty of Medicine, Universitas Tarumanagara, Jakarta, Indonesia; <sup>2</sup>Department of Pharmacology and Therapeutics, Faculty of Medicine, Universitas Indonesia, Jakarta, Indonesia; <sup>3</sup>Department of Medical Pharmacy, Faculty of Medicine, Universitas Indonesia, Jakarta, Indonesia; <sup>4</sup>Department of Biochemistry and Molecular Biology, Faculty of Medicine, Universitas Tarumanagara, Jakarta, Indonesia; <sup>5</sup>Department of Anatomical Pathology, Faculty of Medicine, Universitas Indonesia, Jakarta, Indonesia; <sup>6</sup>Animal Research Facility, IMERI, Faculty of Medicine, Universitas Indonesia, Jakarta, Indonesia; <sup>7</sup>Research Center for Radioisotope, Radiopharmaceutical, and Biodosimetry Technology, Research Organization for Nuclear Energy, National Research and Innovation Agency, Banten, Indonesia

Correspondence: Vivian Soetikno, Department of Pharmacology and Therapeutics, Faculty of Medicine, Universitas Indonesia, Salemba Raya no. 6, Jakarta, 10430, Indonesia, Tel +62 21 31930481, Email vivian.soetikno@ui.ac.id

**Purpose:** Endoplasmic reticulum (ER) stress has a prominent role in the pathogenesis of high-fat diet-induced non-alcohol related fatty liver disease (NAFLD). The aim of this study is to investigate the effects of 6-G on the reduction of ER stress-induced NAFLD in metabolic syndrome (MetS) rats.

**Methods:** Twenty-five male Sprague-Dawley rats were fed with a high-fat high-fructose (HFHF) diet for 16 weeks. The rats were treated orally with 6-G (50, 100, and 200 mg/kgBW) once daily for eight weeks. At Week 16, all animals were sacrificed, and serum and liver tissue were harvested for biochemical and structural analysis.

**Results:** NAFLD liver rats were shown to have elevated protein expression of GRP78, and ER-associated apoptotic protein, such as IRE1, TRAF2, p-JNK, and p-NF-κB, which were considerably reduced by the 6-G at three doses treatment. Furthermore, a significant increase in liver apoptosis and non-alcoholic steatohepatitis (NAS) score were observed in the NAFLD rat liver and which were also attenuated by the 6-G treatment at three doses. 6-G treatment also reduced ALT, AST, and ALP serum levels.

**Conclusion:** Considering all the findings, it is suggested that the 6-G treatment could be a potential candidate therapy in treating ER stress-induced NAFLD in rats.

**Keywords:** 6-gingerol, endoplasmic reticulum, diabetes, insulin resistance, inflammation

## Introduction

Nonalcoholic fatty liver disease (NAFLD) is the hepatic manifestation of metabolic syndrome (MetS). NAFLD is the most common liver disease since its prevalence is estimated to 32.16% in the global population, especially the prevalence in the overweight population is 69.99%.<sup>1</sup> NAFLD includes a spectrum of liver damage, ranging from simple fatty liver disease (NAFL) to nonalcoholic steatohepatitis (NASH), which may progress to cirrhosis.<sup>2</sup> The definitive method for diagnosing NAFLD has relied on liver biopsy, and NAFL is primarily linked to simple steatosis. The primary pathological characteristics of NASH encompass steatosis, hepatocyte ballooning, inflammation, and fibrosis. Therefore, NASH is a progressive form of NAFLD.<sup>3</sup>

The incidence of NAFLD has been shown to be closely correlated with lifestyle. As compared to patients without NAFLD, previous studies showed that patients with NAFLD consumed more foods high in fructose, carbohydrates, and saturated fats. Put another way, the Western diet, which is characterized by a high intake of foods rich in trans fatty acids,

saturated fatty acids, and soft drinks, represents a diet model that is closely related to the incidence of MetS, obesity, hypertension, and type 2 diabetes mellitus.<sup>4-6</sup> A recent study by Im et al has shown that high-fat, high-fructose diets in laboratory animals most strongly mimic the human phenotype of NAFLD.<sup>7</sup> Furthermore, Rohman et al have shown that administering a low dose of streptozotocin (STZ) injection alongside high-fat, high-sucrose diet for 8 weeks in rats can generate MetS that parallels human criteria for the condition.<sup>8</sup>

Endoplasmic reticulum stress has been associated with many liver disorders. This encompasses metabolic disorders including insulin resistance and hepatic steatosis, along with symptoms arising from the interaction of inflammation and metabolic disorders, including steatohepatitis, fibrosis, and cirrhosis.<sup>9</sup> In fact, the ER is crucial for the synthesis, processing, and metabolism of lipids and sterols, serving as the primary organelle for maintaining hepatic lipid homeostasis.<sup>10</sup> Lipid, as a stimulatory signal, is likely to disrupt ER activity. When lipid accumulation, due to excessive intake of high-fat, high-carbohydrate diets, surpasses the metabolic capacity of the endoplasmic reticulum, it triggers a stress response known as ER stress. Endoplasmic reticulum stress induces the activation of the unfolded protein response (UPR), which is facilitated by the transmembrane protein inositol-requiring enzyme 1 alpha (IRE-1 $\alpha$ ), protein kinase R (PKR)-like ER kinase (PERK), and activating transcription factor 6 (ATF6).<sup>11</sup> In a normal condition, these three transmembrane proteins are associated with B-cell immunoglobulin binding protein/glucose-regulated protein 78 (BIP/GRP78) without exposure, making it a crucial regulator of ER homeostasis and stress responses.<sup>12,13</sup> In the context of ER stress, the IRE-1 $\alpha$  pathway functions as the primary mechanism regulating lipogenesis and lipid metabolism by recruiting tumor necrosis factor receptor associated factor 2 (TRAF2) to form IRE-1 $\alpha$ /TRAF2 complex, resulting in the activation of NF- $\kappa$ B signaling.<sup>14</sup> Previous study has demonstrated that GRP78 deletion led to liver lipid accumulation and steatosis.<sup>15</sup> Moreover, it has been shown that IRE-1 $\alpha$ , the most conserved UPR sensor, protects animals from ER stress-induced hepatic steatosis. In fact, sustained interaction between IRE-1 $\alpha$  and TRAF2 leads to activation of JNK and NF- $\kappa$ B, which in turn causes excessive apoptosis and increased inflammatory processes.<sup>16</sup>

Many studies have proved the efficacy of natural products for treating liver disease, such as ginger (*Zingiber officinale* Roscoe). 6-gingerol (6-G) is one of the major phenolic compounds in ginger, which has various biologic activities, such as antioxidant, anti-inflammatory, anti-obese, antidiabetic, and can improve liver function.<sup>17-20</sup> Alsahli et al, have demonstrated the effect of 6-G in lowering AST, ALT and ALP level and the production of pro-inflammatory cytokines as well as oxidative stress in the liver of *Diethylnitrosamine*-induced liver injury in rats.<sup>21</sup> Recent study demonstrated that 6-G could improve NAFLD through activation of the LKB1/AMPK pathway in high-fat diet-fed mice.<sup>22</sup> We have also shown the effect of 6-G in reducing lipid accumulation in hepatic tissue by inhibiting inflammation markers as well as improving beta cell pancreas to increase insulin secretion.<sup>23,24</sup> However, it is not yet known how the mechanism of 6-G improves and/or prevents the progression of NAFL to NASH. Therefore, the current study aims to explore the mechanism of 6-G in overcoming the occurrence of NAFL and NASH through inhibiting ER stress in rats fed a high-fat, high-fructose diet.

## Materials and Methods

### Reagents and Antibodies

6-gingerol (6-G) (CAS: 23513-14-6, HPLC 99.01%) was purchased from Actin Chemicals<sup>®</sup>, Chengdu, China. Streptozotocin (CAS: 18883-66-4) was purchased from Santa Cruz Biotechnology, Texas, USA. Primary antibodies against GRP78 (#3183), (IRE1) (#3294), JNK (#9252), p-JNK (#4668), TRAF2 (#4712), NF- $\kappa$ B (#8242), p-NF- $\kappa$ B (#3033) and GAPDH (#5174) were obtained from Cell-Signaling Technology<sup>®</sup>, Massachusetts, USA. TUNEL Assay Kit – HRP DAB (ab206386) was obtained from Abcam, USA. High-purity grades of all supplementary chemicals in this study were obtained from commercial sources.

### Animals

All the experimental procedures were treated following the Guide for the Care and Use of Laboratory Animals of the National Institutes of Health. This study was approved by the Institutional Animal Care and Use Committee of Universitas Indonesia (approval number: KET-945/UN2.F1/ETIK/PPM.00.02/2021). Eight-week-old male Sprague-

Dawley rats weighing between 180 and 220 grams were procured from the National Agency of Drug and Food Control, Jakarta, Indonesia. The animals were housed in plastic cages in a controlled environment with 65–75% relative humidity at  $21 \pm 2^\circ\text{C}$  and a 12 h light/dark cycle. One cage contains 5 rats. All rats were acclimatized for 1 week before the study.

## Experimental Protocol

The rats were randomly divided into five groups ( $n = 5$  rats per group). Group I served as control-normal (ND) rats fed with a standard pellet diet containing 20% of energy as proteins, 47% of energy as carbohydrates, 4% of energy as lipids, and 29% of energy as minerals (304 kcal/100 g) and water *ad libitum*. The other groups of rats (group II–V) fed with a high-fat high-fructose (HFHF) diet containing 21.31% of energy as proteins, 31.92% of energy as carbohydrates, 29.02% of energy as lipids, and 17.75% of energy as minerals (474 kcal/100 g), and 55% fructose by oral gavage 2 times daily (1.5 mL/day), as previously reported [Munika et al, 2023; Gunawan et al, 2023]. To ensure that each rat in each group received a uniform diet, the diet was weighed every day before administration, namely 20–30 g per animal per day, and the remaining food was weighed again the next day. The composition of the high-fat, high-fructose diet used in our study was established from a previous study that showed it causes MetS in rats [Mutiayani et al, 2014]. After consuming the HFHF diet for eight weeks, streptozotocin (STZ) at a 22 mg/kgBW single dose was injected intraperitoneally after 8-hour fasting. The STZ dosage was determined by our preliminary study, which showed that the optimal dose to induce hyperglycemia in rats without causing death was 22 mg/kgBW. STZ was prepared immediately before injection and dissolved in 0.01 M citrate buffer with pH 4.5. The HFHF diet was continued until Week 16 and 6-G was given to HFHF diet-fed rats after confirmation of the induction of diabetes and its related metabolic disorders, namely fasting plasma glucose  $\geq 250$  mg/dL, plasma triglyceride  $\geq 150$  mg/dL, and obesity (Lee's index  $\geq 300$ ; the formula of Lee's index = body weight [g]<sup>0.33</sup>/naso-anal length [cm]  $\times 10^3$ ). Randomization of the HFHF diet-fed rats was carried out into four treatment groups: HFHF group, 6-G treatment group 50 mg/kg, 100 mg/kg, and 200 mg/kg. 6-G was given by gavage for eight weeks. The maximum dose of 6-G in this study was based on 1/10 of the LD<sub>50</sub> value of ginger, namely 2000 mg/kgBW,<sup>25</sup> while the medium and minimum doses of 6-G were geometric series values of the maximum dose used. At the end of the study (after 16 weeks), all rats were weighed, fasted for 8 hours, anesthetized with ketamine/xylazine (100–2 mg/kg), and sacrificed by exsanguination. Blood from the ventricle was collected for analysis. The liver was stored at  $-80^\circ\text{C}$  until the subsequent analysis. The parts of the remaining excised liver were fixed in 10% formalin.

## Measurement of Biochemical Parameters

The body weights of every animal in each of the five groups were measured once a week to monitor any changes in the animal's total weight, and the data was analyzed appropriately. The Autocheck<sup>®</sup> Glucare glucometer was used to measure fasting serum glucose (Medical Technology Promed, St. Ingbert, Germany). Triglycerides, total serum cholesterol, LDL cholesterol, and HDL cholesterol, AST, ALT and ALP were measured using the colorimetric method (DiaSys Diagnostic Systems GmbH, Holzheim, Germany). The absorbance of the colored solution was measured at 546 nm; the results were, then, interpreted accordingly.

## Western Blotting Analysis

The frozen liver tissues were weighed and homogenized in an ice-cold Tris buffer (50 mm Tris-HCl, pH 7.4; 200 mm NaCl, 20 mm NaF, 1 mm Na<sub>3</sub>VO<sub>4</sub>, 1 mm 2-mercaptoethanol; 0.01 mg/mL leupeptin; 0.01 mg/mL aprotinin). Then, samples were centrifuged at 3000 rpm for 10 min at  $4^\circ\text{C}$ , and supernatants were collected and stored at  $-80^\circ\text{C}$  until analysis. The bicinchoninic acid (BCA) technique was used to assess the sample's total protein content. Equal volumes of protein extract (50  $\mu\text{g}$ ) were separated by sodium dodecyl sulphate polyacrylamide gel electrophoresis (SDS-PAGE) (Bio-Rad, CA, USA) and electrophoretically transferred to nitrocellulose membranes for the purpose of determining the protein levels of GRP78; IRE-1; TRAF2; p-JNK; and p-NF- $\kappa\text{B}$ . The next step was blocking the membranes using 5% non-fat skim milk in Tris buffered saline Tween (20 mm Tris pH 7.6, 137 mm NaCl, and 0.1% Tween 20). All the antibodies were used at a dilution of 1:1000. The membrane was then incubated overnight at  $4^\circ\text{C}$  with the primary antibody, and the bound antibody was visualized using the respective horse-radish peroxidase-conjugated secondary antibodies (Cell Signaling Inc., Beverly, MA, USA) and chemiluminescence developing agents (Bio-Rad Laboratories

Inc, Hercules, CA, USA). The level of GAPDH was estimated in every sample to ensure the equal protein loading of the samples. The films were scanned, and the band densities were quantified with ImageJ analysis.

## Light Microscopic Morphological Study

All the liver tissue samples were fixed in 10% neutral buffer formalin solution and paraffin embedded block was made. After thin sectioning (4  $\mu\text{m}$ ), the sections were mounted on slides. The hematoxylin and eosin (H&E) staining was performed to examine the architecture of liver tissues. Histopathological examination was performed by using a light microscope (Olympus, Tokyo, Japan) and the slides figures were shot accordingly. The histological findings were performed by double-blinded histopathologist. For each animal, five sections were scored for steatosis, hepatocyte ballooning, lobular inflammation, and NAS scores. The severity of steatosis was graded based on the percentage of the total area affected into the following categories: 0 (<5%), 1 (5–33%), 2 (34–66%), and 3 (>66%). Likewise, the level of hepatocyte ballooning was scored based on the percentage of the total area affected, into the following categories: 0 (<5%), 1 (5–33%), 2 (34–66%), and 3 (>66%). Lobular inflammation was evaluated by counting the number of inflammatory foci per field and was categorized as follows: 0 (<0.5 foci), 1 (0.5–1.0 foci), 2 (1.0–2.0 foci), and 3 (>2.0 foci). Grading for NAS score was based on steatosis and inflammation as follows: 0 (steatosis <5% and inflammation <0.5 foci/field), 1 (steatosis 5–33% and inflammation 0.5–1.0 foci/field), 2 (steatosis 33–66% and inflammation 1.0–2.0 foci/field), and 3 (steatosis >66% and inflammation >2.0 foci/field).<sup>26</sup>

## Terminal Deoxynucleotidyl Transferase (TdT)-Mediated dUTP Nick-End-Labeling (TUNEL) Staining

Formalin sections embedded in paraffin were stained with TUNEL using the TUNEL Assay Kit-HRP-DAB (Abcam; ab206386) in accordance with the manufacturer's instructions. Five sections were graded for apoptotic nuclei in each animal. The nucleus' brown color intensity was used to identify the apoptotic cells. The percentage of apoptotic cells divided by the total number of cells in each field of view is known as the apoptotic index.

## Statistical Analysis

Data are represented as the mean  $\pm$  SD. Multiple comparisons were performed by one-way ANOVA test and Tukey's post hoc test to ascertain control group and treatment groups. SPSS ver. 21 was used to perform the statistical analysis. Differences were considered significant at  $p < 0.05$ .

## Results

### 6-Gingerol Administration Reduces Body Weight Gain and Liver Weight/Body Weight Ratio in HFHF Diet-Fed Rats

A significant increase of liver size, body weight (BW), liver weight (LW), and LW/BW ratio were observed in rats after HFHF diet for 16 weeks when compared with ND rats (Figure 1A-D). The macroscopic features of the liver of HFHF diet-fed rats showed that the edges were blunt, brittle, yellowish in color and had a nodular appearance (Figure 1A, HFHF). Importantly, 6-G administration at three doses was associated with significantly reduced body weight ( $p < 0.05$  for 6-G 100 and 6-G 200), LW/BW ratio ( $p < 0.01$  for all three doses of 6-G) and improved smoother appearance of liver without nodularity (Figure 1A-D).

### Effect of 6-Gingerol on Liver Enzymes and Serum Lipid Profile

A significant increase in liver enzyme including ALT ( $p < 0.01$ ), AST ( $p < 0.05$ ), and ALP ( $p < 0.01$ ) were shown in HFHF diet-fed rats as compared to that of ND-fed rats (Table 1). The administration of 6-G at all three doses can significantly lower AST, ALT, and ALP levels compared to the HFHF group, although the 6-G dose of 50 mg/kg/day demonstrated a reduction in these levels approaching normal ranges. The levels of triglyceride, total cholesterol, and LDL-C in the HFHF diet-fed rats showed a significant increase compared with the ND diet-fed rats after 16 weeks of receiving HFD ( $p < 0.01$ ) (Figure 2A-C), whereas there was no difference in the level of HDL-C in all groups

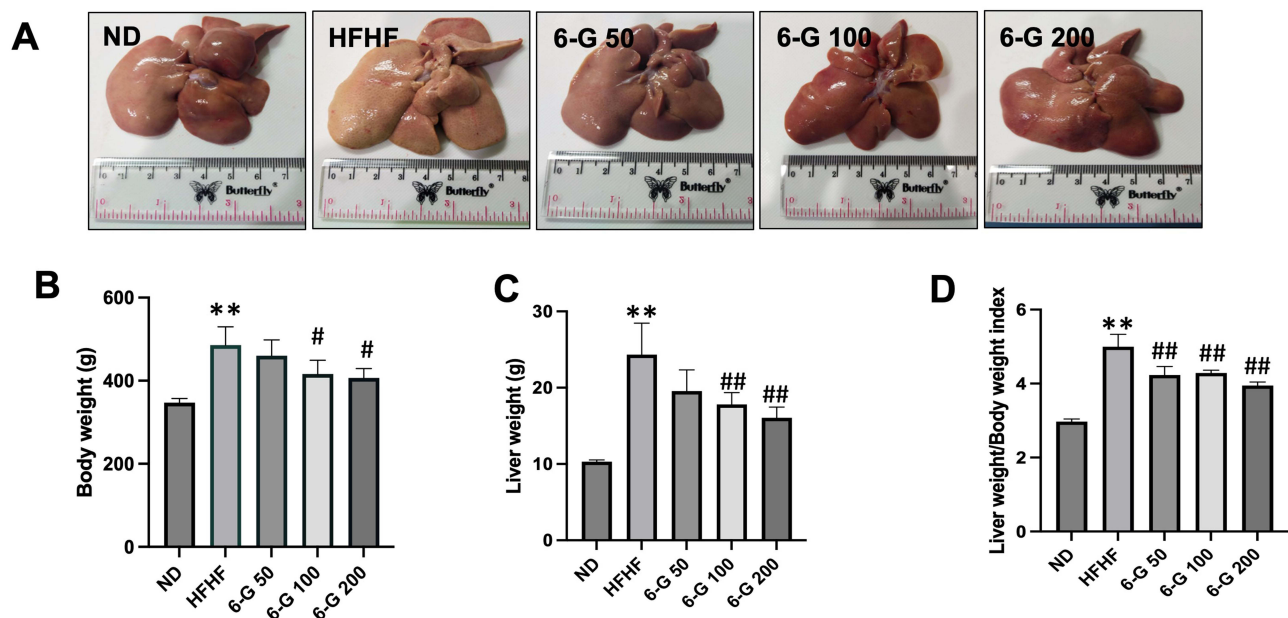


**Figure 1** The effect of HFHF alone or in combination with 6-gingerol doses of 50, 100, and 200 mg/kg/day on (A) liver tissue morphology, (B) Body weight, (C) Liver weight, and (D) Liver weight to body weight ratio. All values are presented as the mean  $\pm$  SD;  $n = 5$ ; \*\* $p < 0.01$  vs ND, # $p < 0.05$  and ### $p < 0.01$  vs HFHF.

(Figure 2D). After administering 6-G at all three doses, serum lipid profile, namely triglyceride, total cholesterol, and LDL-C decreased significantly to the levels of the ND diet-fed rats.

### Effect of 6-Gingerol on the ER Stress in the Liver of HFHF Diet-Fed Rats

The effect of 6-gingerol on the ER stress pathway was observed by Western blot analysis of the expression of NAFLD liver rat proteins GRP78, IRE1, TRAF2, JNK, and NF- $\kappa$ B. The protein expression of GRP78, an indicator for the induction of ER stress, in the HFHF diet-fed rats was significantly increased when compared with the ND diet-fed rats ( $p < 0.01$ ) (Figure 3A). These results align with the findings for the IRE1 and TRAF2 proteins, in which the protein expression of IRE1 and TRAF2 were significantly increased in the HFHF-fed rats when compared to the ND diet-fed rats ( $p < 0.01$ ) (Figure 3B and C). In addition, the NAFLD liver's rats were shown significant increment in the protein expression of phosphorylation of JNK ( $p < 0.01$ ) as well as NF- $\kappa$ B ( $p < 0.05$ ) (Figure 3D and E). Interestingly, 6-G-treated rats at all three doses were found to have attenuated protein expression of GRP78, IRE1, TRAF2, p-JNK, and p-NF- $\kappa$ B in NAFLD rats in comparison to HFHF diet-fed rats, mainly at a dose of 200 mg/kg/day (Figure 3A-E).

### Effects of 6-Gingerol on Hepatic Steatosis

The HFHF diet-fed rats showed obvious hepatic steatosis, as demonstrated by the hematoxylin and eosin staining of paraffin tissue sections (Figure 4A). This was in accordance with the results of quantitative analysis scoring of steatosis (Figure 4B), hepatocyte ballooning (Figure 4C), lobular inflammation (Figure 4D), and NAS (Figure 4E). Administration of 6-G at doses of 100 and 200 mg/kgBW/day for 8 weeks significantly improved the condition of hepatic steatosis, as

**Table 1** Effect of 6-Gingerol on Hepatic Enzyme Function ( $n = 5$  Rats/Group)

Parameters	ND	HFHF	6-G 50	6-G 100	6-G 200
AST (mg/dL)	60.49 $\pm$ 13	84.11 $\pm$ 19.7 <sup>#</sup>	59.93 $\pm$ 40.3	47.36 $\pm$ 13.8*	66.19 $\pm$ 15.5
ALT (mg/dL)	35 $\pm$ 4.9	286.47 $\pm$ 62.7 <sup>###</sup>	42.05 $\pm$ 12.7 <sup>**</sup>	44.77 $\pm$ 16.5 <sup>**</sup>	46.91 $\pm$ 23.4 <sup>**</sup>
ALP (mg/dL)	229.16 $\pm$ 19.6	549.3 $\pm$ 155.4 <sup>###</sup>	291.36 $\pm$ 57.9*	358.28 $\pm$ 52*	322.29 $\pm$ 75.6*

Notes: # $p < 0.05$  vs ND. ### $p < 0.01$  vs ND. \* $p < 0.05$  vs HFHF. \*\* $p < 0.01$  vs HFHF.

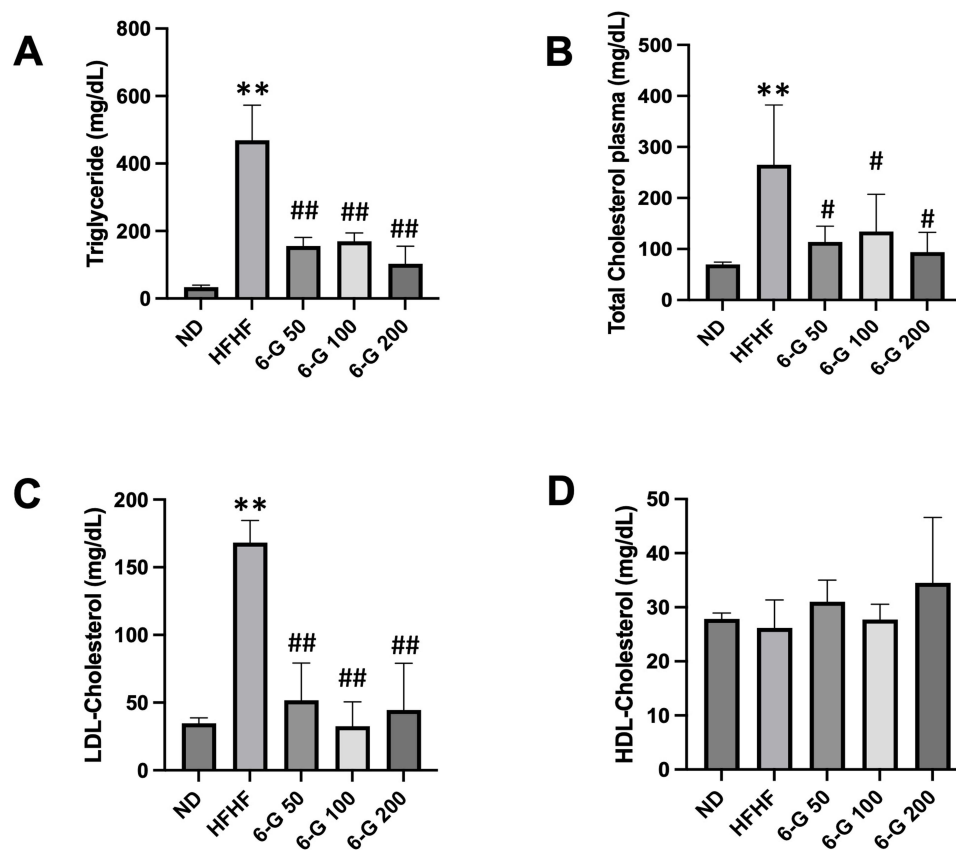


**Figure 2** The effect of HFHF alone or in combination with 6-gingerol doses of 50, 100, and 200 mg/kg/day on serum lipid profile. (A) Triglyceride, (B) Total cholesterol, (C) LDL cholesterol, (D) HDL cholesterol. All values are presented as the mean  $\pm$  SD;  $n = 5$ ; \*\* $p < 0.01$  vs ND, # $p < 0.05$  and ## $p < 0.01$  vs HFHF.

indicated by a reduction in steatosis, lobular inflammation, hepatocyte ballooning, and NAS scores in the 6-G-treated HFHF diet-fed rats as compared to the HFHF diet-fed rats (Figure 4A-E).

## Effects of 6-Gingerol on the Liver Apoptosis

To assess the liver apoptosis in HFHF diet-fed rats, we employed TUNEL assay, which revealed that the NAFLD rats were found to have increased liver apoptotic nuclei, in comparison to ND diet-fed rats and administration of 6-G at all three doses for 8 weeks were found to have less liver apoptotic nuclei in NAFLD rats (Figure 5A and B).

## Discussion

In the current investigation, rats were fed a high-fat high-fructose diet (HFHF) for 16 weeks, which is a well-established model for the development of non-alcoholic related fatty liver disease (NAFLD).<sup>27</sup> This is also related to clinical study in which poor dietary habits were the primary problem in NAFLD.<sup>28</sup> Long-term studies have shown that the rising of ER stress is correlated with the occurrence of NAFLD, namely the downregulation of IRE1, ATF6, and EIF2S1 protein expression.<sup>29</sup> The data reported in this study revealed that HFHF diet for 16 weeks caused elevation in lipid plasma, hepatocyte steatosis, hepatocyte ballooning, lobular inflammation, NAS score, and liver apoptosis as well as elevation of ER stress-associated protein markers, such as GRP78, IRE1, TRAF2, p-JNK, and p-NF- $\kappa$ B. In addition to preventing HFHF-induced NAFLD, treatment with 6-G at doses of 50, 100, and 200 mg/kg/day for 8 weeks ameliorated ER stress in the liver of HFHF diet-fed rats.

Excessive intake of fat and carbohydrate causes lipid accumulation in liver, leading to NAFLD.<sup>30</sup> Endoplasmic reticulum is an important organelle for metabolizing hepatic lipids, including synthesis, storage, and export of lipids. The UPR, a highly conserved pathway in ER, monitors protein synthesis, lipid metabolism, and maintain ER homeostasis.<sup>31</sup>

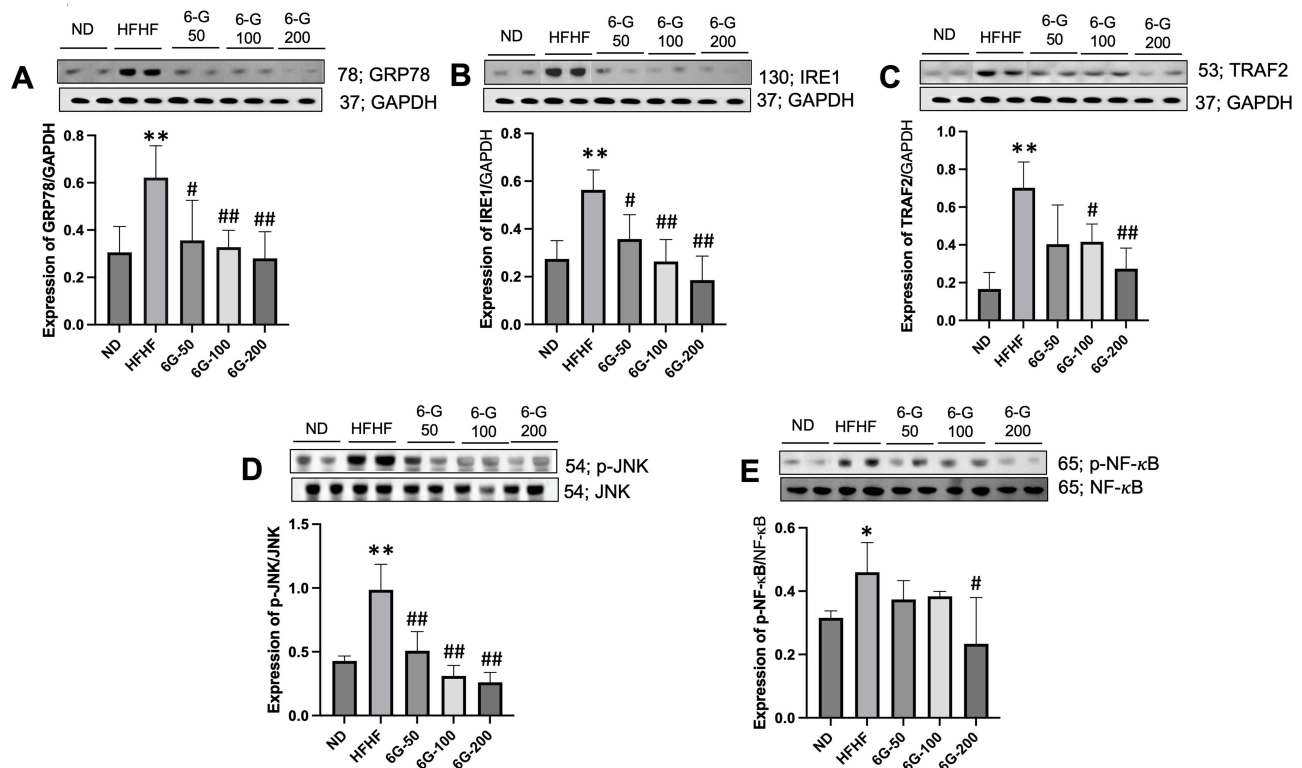


**Figure 3** The effect of HFHF alone or in combination with 6-gingerol doses of 50, 100, and 200 mg/kg/day on the liver expression of (A) GRP78, (B) IRE1, (C) TRAF2, (D) p-JNK, and (E) p-NF-κB in rats. A representative Western blot showing specific bands for each protein parameter of ER stress with GAPDH as an internal control was quantified using densitometric analysis. An equal amount of protein sample obtained from liver homogenate was applied to each lane. All values are presented as the mean  $\pm$  SD;  $n = 5$ ; \* $p < 0.05$  and \*\* $p < 0.01$  vs ND, # $p < 0.05$  and ### $p < 0.01$  vs HFHF.

Notably, lipid overload causes ER stress in the liver, not only in humans but also in experimental animals, which in turn causes chronic activation of UPR, oxidative stress, apoptosis, and inflammation.<sup>32,33</sup> It has been reported that hepatic steatosis and insulin resistance in obese mice are closely related to ER stress, and GRP78 plays a crucial role in the control of ER homeostasis and stress responses, because it interacts and sequesters all key UPR sensors.<sup>34</sup> In this study, we have found that the NAFLD liver rats had significant increase in the protein expression of GRP78 in comparison to standard diet-fed rats and 6-G treatment at three doses significantly attenuated those protein expression level in NAFLD liver rats. In line with our study, Yun and Lee (2022) have demonstrated that gingerol administration in tunicamycin-induced HepG2 cells decreased the mRNA expression of ER stress markers, including GRP78 and IRE1.<sup>35</sup> Conversely, previous studies have suggested that overexpression of GRP78 inhibited ER stress-induced steatosis in the liver and deletion of GRP78 led to ER stress and apoptosis.<sup>15,36</sup> The reason for these contradictory results is poorly understood.

IRE1, one of the UPR sensors, is an important pathway in the upregulation of inflammation, apoptosis, and tissue remodelling.<sup>37,38</sup> In fact, IRE1 and TRAF2 interaction activates JNK pathways, which are important for the upregulation of apoptosis.<sup>39</sup> 6-G administration, mainly at doses of 100 and 200 mg/kg/day leads to a lower protein expression of IRE1, TRAF2, and p-JNK significantly as compared to the HFHF diet-fed rats. Moreover, 6-G significantly reduced the number of apoptotic cells in the liver tissues of HFHF diet-fed rats. Our results are consistent with those of Yi et al, where 6-shogaol, one of the bioactive compounds of ginger other than 6-gingerol, reduced the levels of apoptotic cells in the liver of diabetic mice.<sup>40</sup> In addition, Ma and Lee (2022) have also shown that ginger extract inhibits apoptosis in diabetic retinopathy rats.<sup>41</sup> Conversely, in tumor cells, 6-gingerol has been reported to induce apoptosis, exhibit cell-cycle arrest and enzyme-coupled cell signaling receptor degeneration in cancer cells.<sup>18,42,43</sup> This suggests that 6-gingerol can act as antiapoptotic and apoptotic in non-tumor cells and tumor cells, respectively.

NAFLD involves a range of conditions associated with the accumulation of triglycerides in hepatocytes, ranging from isolated hepatic steatosis to progressive non-alcoholic steatohepatitis (NASH), which may result in cirrhosis and

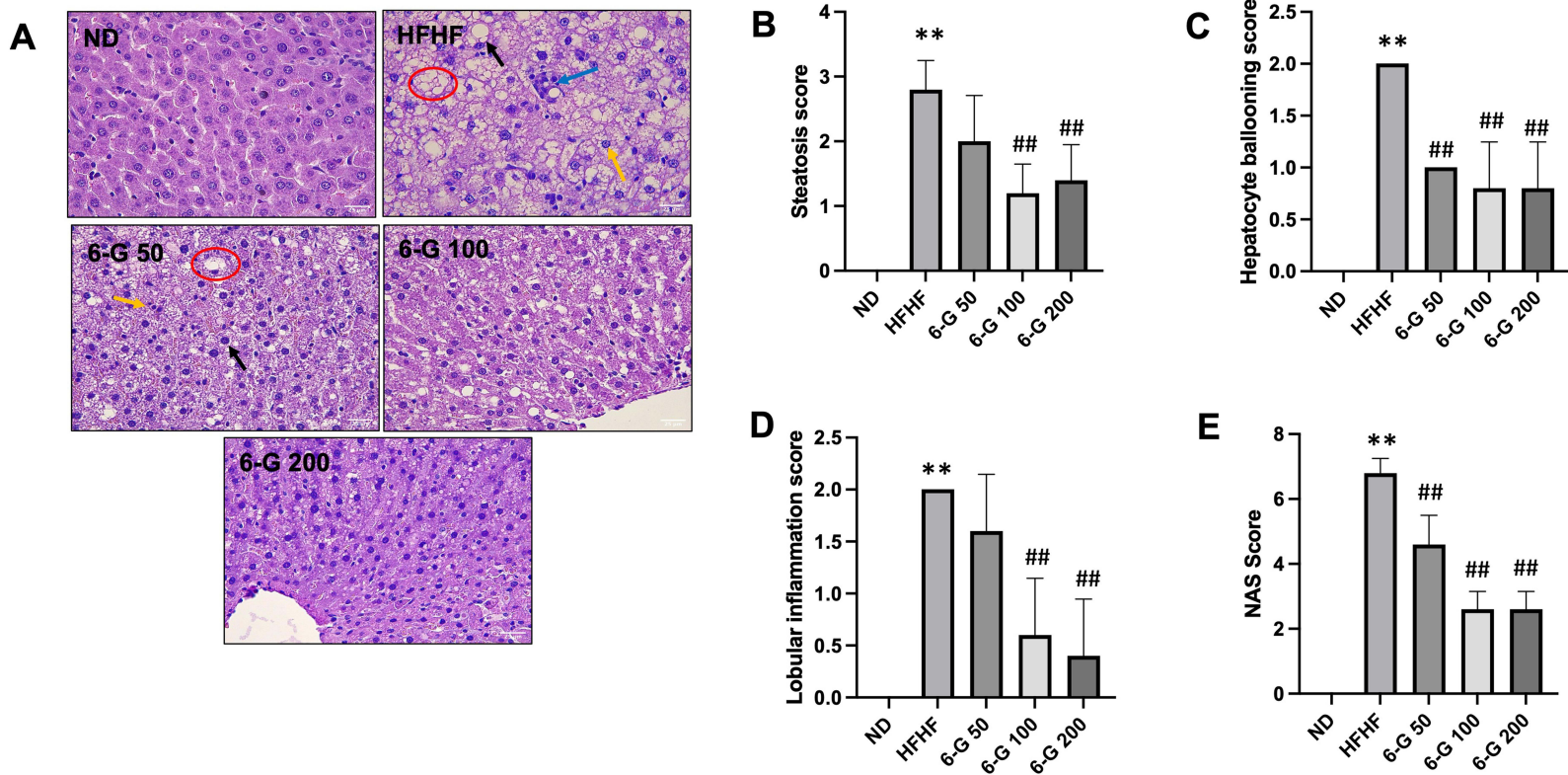


**Figure 4** (A) Histopathology of the liver from ND diet-fed rats, HFHF diet-fed rats or in combination with 6-gingerol doses 50, 100, and 200 mg/kg/day. ND rats showed normal architecture of hepatocytes. HFHF diet-fed rats caused macrovesicular steatosis (black arrow), microvesicular steatosis (yellow arrow), lobular inflammation (blue arrow), and hypertrophied cells (red circle). 6-gingerol-treated HFHF-challenged rat at all three doses showed improvement of architecture of hepatocytes almost similar to ND rats. Magnification x 200. Semi-quantitative analysis of liver steatosis score (B), hepatocyte ballooning score (C), lobular inflammation score (D), and NAS score (E) in each group. All values are presented as the mean ± SD;  $n = 5$ ; \*\* $p < 0.01$  vs ND, ## $p < 0.01$  vs HFHF.



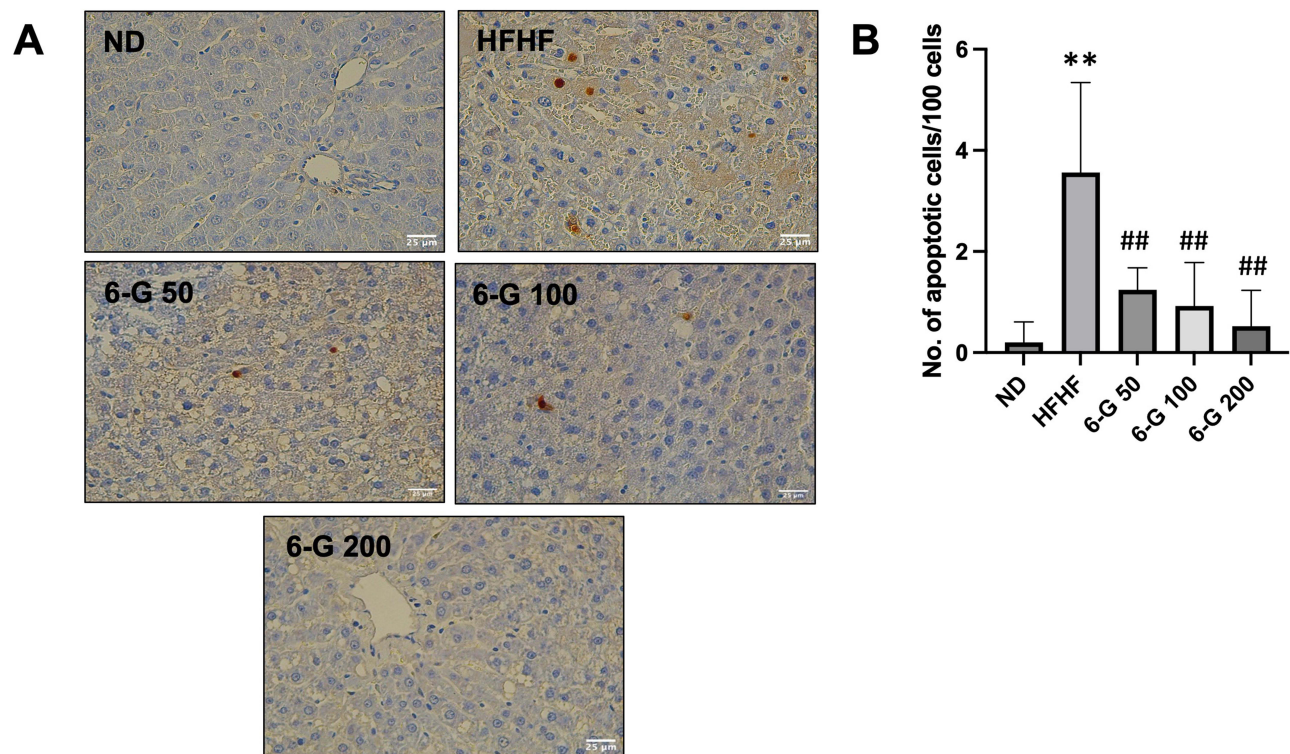


**Figure 5 (A)** Representative TUNEL-stained image of liver tissue from each group. **(B)** Semi-quantitative bar graphs of percentage of liver apoptotic nuclei in the HFHF alone or in combination with 6-gingerol doses of 50, 100, and 200 mg/kg/day. Magnification x 400. All values are presented as the mean  $\pm$  SD;  $n = 5$ ; \*\* $p < 0.01$  vs ND, ## $p < 0.01$  vs HFHF.

progressive liver damage.<sup>44</sup> One of the mechanisms proposed that underlying the progression from isolated hepatic steatosis to NASH is ER stress and dysregulated of UPR proteins.<sup>16,45,46</sup> In fact, NASH is associated with increased IRE1 and its interactions with TRAF2 to promote NF- $\kappa$ B activation and inflammatory response.<sup>47</sup> In the current study, we have shown that the administration of 6-gingerol at all three doses reduced liver NF- $\kappa$ B protein expression, although only at a dose of 200 mg/kg/day showed a statistically significant difference compared to HFHF diet-fed rats, which further inhibited lobular inflammation and hepatocyte ballooning as well as prevented the progression of NAFL to NASH. Our findings were in line with Wong et al<sup>48</sup> and Tzeng et al<sup>20</sup> who found the same results in metabolic syndrome rat model. Recent study also showed that 6-G improved HFD-induced NAFLD in rats through increasing the activity of the LKB1/AMPK pathway.<sup>22</sup> Furthermore, gingerol contained in kimchi can suppress ER stress in tunicamycin-induced mice and in vitro by increasing AMPK activity.<sup>35</sup> This suggests that 6-G can ameliorate ER stress through its synergistic effects with other pathways.

In our study, we also observed that 6-G at a dose of 200 mg/kg/day for 8 weeks was able to improve all NAFLD-related parameters induced by the HFHF diet, with no apparent dose-dependency of 6-G in any of the parameters examined. In contrast, Sampath et al demonstrated that 6-G intraperitoneally at dosage of 25 mg/kg/day and 75 mg/kg/day resulted in dose-dependency reductions in insulin, AST, ALT, and blood glucose levels in obese mice.<sup>49</sup> Therefore, to prove whether there is dose-dependence of 6-G requires further research.

## Conclusion

Based on the above results, it is concluded that prolonged consumption of the HFHF diet appears to be promoting the development of NAFLD and raising the possibility that it may advance to NASH via the up regulation of ER stress and UPR activation. 6-G, mainly at a dose of 200 mg/kg/day, decreased ER stress-related NAFLD and prevented the progression of NAFLD into NASH (Figure 6). These results were followed by improvements in lipid serum, including decreased triglyceride, total cholesterol, and LDL cholesterol. Therefore, 6-G is a promising drug candidate for further development

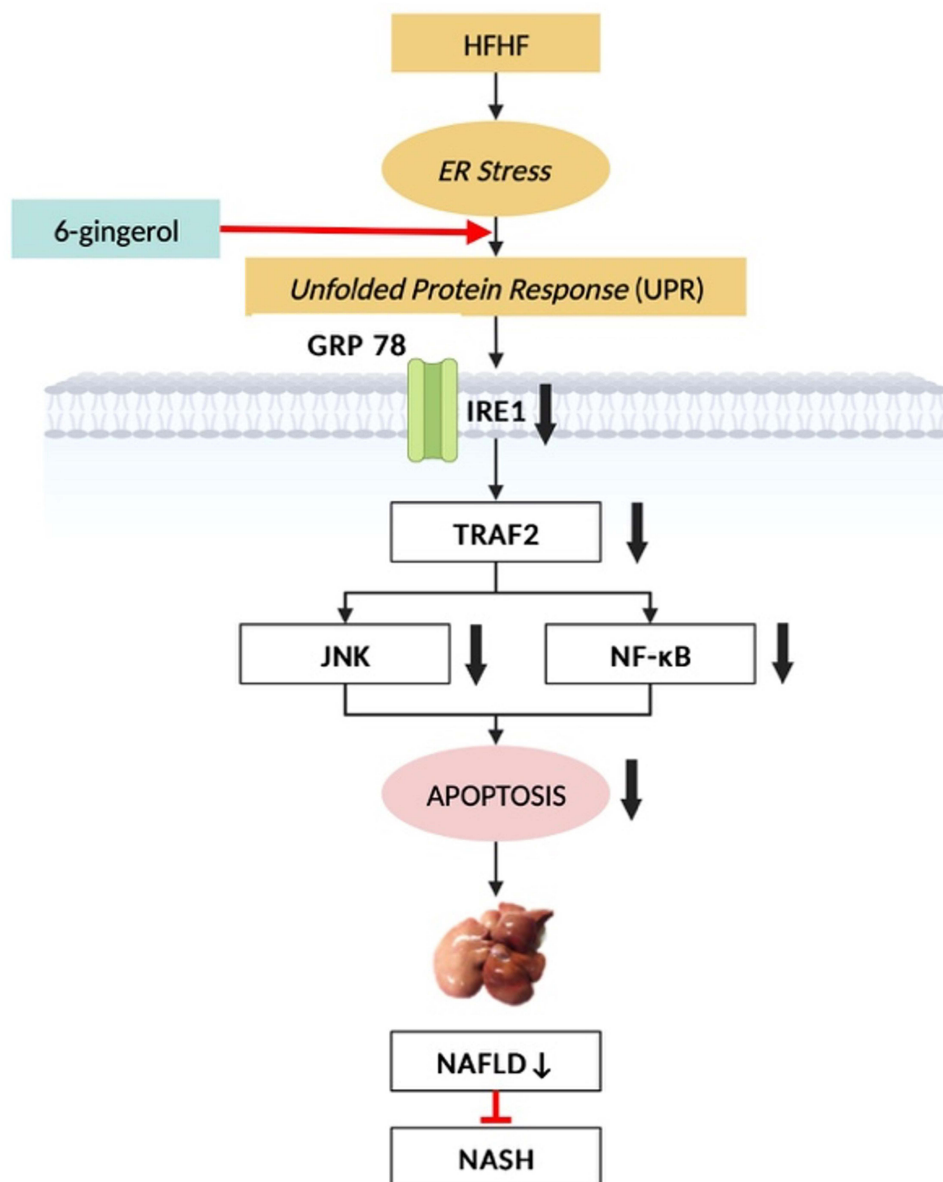


**Figure 6** Proposed mechanism of action of 6-gingerol in ameliorating non-alcoholic related fatty liver disease in rats.

as a therapy to treat NAFLD. Nevertheless, this study presents certain limitations: firstly, we administered 6-G for a duration of up to 8 weeks, which restricts our understanding of the dose-dependency of potential long-term effects and outcomes. The second limitation is that toxicity studies have not been conducted to determine the  $LD_{50}$  of the 6-G currently used; understanding the kinetic relationship between the blood level produced and the administered dose of 6-G is crucial for identifying the safe dose range and dose-dependency. However, this study may serve as a reference for future research on humans with metabolic syndrome, a condition that presently necessitates multiple pharmacological interventions.

## Acknowledgment

We thank to Chiswytta Chaliana and Annisa Ulhuriyah for their technical assistance.

## Funding

This study was supported by a research grant from Ministry of Education, Culture, Research, and Technology of the Republic of Indonesia with a grant number NKB-868/UN2.RST/HKP.05.00.2024. We thank our laboratory staff for supporting the study.

## Disclosure

The authors report no conflicts of interest in this work.

## References

1. Younossi ZM, Golabi P, Paik JM, et al. The global epidemiology of nonalcoholic fatty liver disease (NAFLD) and nonalcoholic steatohepatitis (NASH): a systematic review. *Hepatology*. 2023;77(4):1335–1347. doi:10.1097/HEP.0000000000000004
2. Carreres L, Jilkova ZM, Vial G, Marche PN, Decaens T, Lerat H. Modeling diet-induced NAFLD and NASH in rats: a comprehensive review. *Biomedicines*. 2021;9(4):1–16. doi:10.3390/biomedicines9040378
3. Loomba R, Friedman SL, Shulman GI. Mechanisms and disease consequences of nonalcoholic fatty liver disease. *Cell*. 2021;184(10):2537–2564. doi:10.1016/j.cell.2021.04.015
4. Wehmeyer MH, Zyriax BC, Jagemann B, et al. Nonalcoholic fatty liver disease is associated with excessive calorie intake rather than a distinctive dietary pattern. *Medicine*. 2016;95(23):e3887. doi:10.1097/MD.0000000000003887
5. Alferink LJ, Kieft-de Jong JC, Erler NS, et al. Association of dietary macronutrient composition and non-alcoholic fatty liver disease in an ageing population: the Rotterdam study. *Gut*. 2019;68(6):1088–1098. doi:10.1136/gutjnl-2017-315940
6. Coronati M, Baratta F, Pastori D, et al. Added fructose in non-alcoholic fatty liver disease and in metabolic syndrome: a narrative review. *Nutrients*. 2022;14(6):1127. doi:10.3390/nu14061127
7. Im YR, Hunter H, de Gracia Hahn D, et al. A systematic review of animal models of NAFLD finds high-fat, high-fructose diets most closely resemble human NAFLD. *Hepatology*. 2021;74(4):1884–1901. doi:10.1002/hep.31897
8. Rohman MS, Lukitasari M, Nugroho DA, et al. Development of an experimental model of metabolic syndrome in Sprague Dawley rat. *Res J Life Sci*. 2017;4(1):76–86. doi:10.21776/ub.rjls.2017.004.01.10
9. Nogueira JP, Cusi K. Role of insulin resistance in the development of nonalcoholic fatty liver disease in people with type 2 diabetes: from bench to patient care. *Diabetes Spectr*. 2024;37(1):20–28. doi:10.2337/dsi23-0013
10. Rennert C, Heil T, Schicht G, et al. Prolonged lipid accumulation in cultured primary human hepatocytes rather leads to ER stress than oxidative stress. *Int J Mol Sci*. 2020;21(19):7097. doi:10.3390/ijms21197097
11. Mohan S, Rani MRP, Brown L, Ayyappan P, Raghu KG. Endoplasmic reticulum stress: a master regulator of metabolic syndrome. *Eur J Pharmacol*. 2019;860:1–10. doi:10.1016/j.ejphar.2019.172553
12. Jiang Q, Sun Y, Guo Z, et al. Overexpression of GRP78 enhances survival of CHO cells in response to serum deprivation and oxidative stress. *Eng Life Sci*. 2016;17(2):107–116. doi:10.1002/elsc.201500152
13. Pfaffenbach KT, Lee AS. The critical role of GRP78 in physiologic and pathologic stress. *Curr Opin Cell Biol*. 2011;23(2):150–156. doi:10.1016/j.ceb.2010.09.007
14. Riaz TA, Junjappa RP, Handigund M, et al. Role of endoplasmic reticulum stress sensor ire1 $\alpha$  in cellular physiology, calcium, ros signaling, and metaflammation. *Cells*. 2020;9(5):1160. doi:10.3390/cells9051160
15. Ji C, Kaplowitz N, Lau MY, et al. Liver-specific loss of glucose-regulated protein 78 perturbs the unfolded protein response and exacerbates a spectrum of liver diseases in mice. *Hepatology*. 2011;54(1):229–239. doi:10.1002/hep.24368
16. Zhang K, Wang S, Malhotra J, et al. The unfolded protein response transducer IRE1 $\alpha$  prevents ER stress-induced hepatic steatosis. *EMBO J*. 2011;30(7):1357–1375. doi:10.1038/emboj.2011.52
17. Choy KW, Murugan D, Mustafa MR. Natural products targeting er stress pathway for the treatment of cardiovascular diseases. *Pharmacol Res*. 2018;132:119–129. doi:10.1016/j.phrs.2018.04.013
18. Mao QQ, Xu XY, Cao SY, et al. Bioactive compounds and bioactivities of ginger (zingiber officinale roscoe). *Foods*. 2019;8(6):1–21. doi:10.3390/foods8060185
19. Rahimlou M, Yari Z, Rayyani E, et al. Effects of ginger supplementation on anthropometric, glycemic and metabolic parameters in subjects with metabolic syndrome: a randomized, double-blind, placebo-controlled study. *J Diabetes Metab Disord*. 2019;18(1):119–125. doi:10.1007/s40200-019-00397-z
20. Tzeng TF, Liou SS, Chang CJ, et al. 6-gingerol protects against nutritional steatohepatitis by regulating key genes related to inflammation and lipid metabolism. *Nutrients*. 2015;7(2):999–1020. doi:10.3390/nu7020999
21. Alsahli MA, Almatroodi SA, Almatroudi A, et al. 6-gingerol, a major ingredient of ginger attenuates diethylnitrosamine-induced liver injury in rats through the modulation of oxidative stress and anti-inflammatory activity. *Mediators Inflamm*. 2021;2021:1–17. doi:10.1155/2021/6661937
22. Liu Y, Li D, Wang S, et al. 6-gingerol ameliorates hepatic steatosis, inflammation and oxidative stress in high-fat diet-fed mice through activating LKB1/AMPK Signaling. *Int J Mol Sci*. 2023;24(7):6285. doi:10.3390/ijms24076285
23. Gunawan S, Munika E, Wulandari ET, et al. 6-gingerol ameliorates weight gain and insulin resistance in metabolic syndrome rats by regulating adipocytokines. *Saudi Pharm J*. 2023;31(3):351–358. doi:10.1016/j.jsps.2023.01.003
24. Munika E, Gunawan S, Wuyung PE, et al. Beneficial effects of 6-gingerol on fatty pancreas disease in high-fat high-fructose diet-induced metabolic syndrome rat model. *Pancreas*. 2023;53(2):e193–e198. doi:10.1097/MPA.0000000000002287
25. Benny M, Shylaja MR, Antony B, et al. Acute and subacute toxicity studies with ginger extract in rats. *Int J Pharm Sci Res*. 2020;12:2799–2809. E-ISSN: 0975-8232.
26. Liang W, Menke AL, Driessen A, et al. Establishment of a general NAFLD scoring system for rodent models and comparison to human liver pathology. *PLoS One*. 2014;9(12):e115922. doi:10.1371/journal.pone.0115922

27. Zarghani SS, Soraya H, Zarei L, et al. Comparison of three different diet-induced non-alcoholic fatty liver disease protocols in rats: a pilot study. *Pharm Sci.* 2016;22(1):9–15. doi:10.15171/PS.2016.03
28. Brunt EM, Wong VW, Nobili V, et al. Nonalcoholic fatty liver disease. *Nat Rev Dis Primers.* 2015;1(1):15080. doi:10.1038/nrdp.2015.80
29. Li Z, Yu H, Li Y. Identification of key endoplasmic reticulum stress-related genes in non-alcoholic fatty liver disease. *Bio Med Informatics.* 2022;3:424–433. doi:10.3390/biomedinformatics2030027
30. Parry SA, Hodson L. Influence of dietary macronutrients on liver fat accumulation and metabolism. *J Investig Med.* 2017;65(8):1102–1115. doi:10.1136/jim-2017-000524
31. Hariri N, Thibault L. High-fat diet-induced obesity in animal models. *Nutr Res Rev.* 2010;23(2):270–299. doi:10.1017/S0954422410000168
32. Wang P, Lu Z, He M, et al. The effects of endoplasmic-reticulum-resident seleno proteins in a nonalcoholic fatty liver disease pig model induced by a high-fat diet. *Nutrients.* 2020;12(3):692. doi:10.3390/nu12030692
33. Lei N, Song H, Zeng L, et al. Persistent lipid accumulation leads to persistent exacerbation of endoplasmic reticulum stress and inflammation in progressive NASH via the IRE1 $\alpha$ /TRAF2 complex. *Molecules.* 2023;28(7):3185. doi:10.3390/molecules28073185
34. Chen WT, Zhu G, Pfaffenbach K, et al. GRP78 as a regulator of liver steatosis and cancer progression mediated by loss of the tumor suppressor PTEN. *Oncogene.* 2014;33(42):4997–5005. doi:10.1038/ncr.2013.437
35. Yun YR, Lee JE. Alliin, capsaicin, and gingerol attenuate endoplasmic reticulum stress-induced hepatic steatosis in HepG2 cells and C57BL/6N mice. *J Funct Foods.* 2022;95:105186. doi:10.1016/j.jff.2022.105186
36. Kammoun HL, Chabanon H, Hainault I, et al. GRP78 expression inhibits insulin and ER stress-induced SREBP-1c activation and reduces hepatic steatosis in mice. *J Clin Invest.* 2009;119(5):1201–1215. doi:10.1172/JCI37007
37. Huang R, Hui Z, Wei S, et al. IRE1 signaling regulates chondrocyte apoptosis and death fate in the osteoarthritis. *J Cell Physiol.* 2022;237(1):118–127. doi:10.1002/jcp.30537
38. Tam AB, Mercado EL, Hoffmann A, et al. ER stress activates NF- $\kappa$ B by integrating functions of basal IKK activity, IRE1 and PERK. *PLoS One.* 2012;7(10):e45078. doi:10.1371/journal.pone.0045078
39. Guo B, Li Z. Endoplasmic reticulum stress in hepatic steatosis and inflammatory bowel diseases. *Front Genet.* 2014;5:242. doi:10.3389/fgene.2014.00242
40. Yi JK, Ryou ZY, Ha JJ, et al. Beneficial effects of 6-shogaol on hyperglycemia, islet morphology and apoptosis in some tissues of streptozotocin-induced diabetic mice. *Diabetol Metab Syndr.* 2019;11(1):15. doi:10.1186/s13098-019-0407-0
41. Ma H, Li J. The ginger extract could improve diabetic retinopathy by inhibiting the expression of eNOS and G6PDH, apoptosis, inflammation, and angiogenesis. *J Food Biochem.* 2022;46(5):e14084. doi:10.1111/jfbc.14084
42. Tsai Y, Xia C, Sun Z. The inhibitory effect of 6-gingerol on ubiquitin-specific peptidase 14 enhances autophagy-dependent ferroptosis and anti-tumor *in vivo* and *in vitro*. *Front Pharmacol.* 2020;11:598555. doi:10.3389/fphar.2020.598555
43. Huang P, Zhou P, Liang Y, et al. Exploring the molecular targets and mechanisms of [10]-Gingerol for treating triple-negative breast cancer using bioinformatics approaches, molecular docking and *in vivo* experiments. *Transl Cancer Res.* 2021;10(11):4680–4693. doi:10.21037/tcr-21-1138
44. Liu X, Green RM. Endoplasmic reticulum stress and liver diseases. *Liver Res.* 2019;3(1):55–64. doi:10.1016/j.livres.2019.01.002
45. Lake AD, Novak P, Hardwick RN, et al. The adaptive endoplasmic reticulum stress response to lipotoxicity in progressive human nonalcoholic fatty liver disease. *Toxicol Sci.* 2014;137(1):26–35. doi:10.1093/toxsci/kft230
46. Lee S, Kim S, Hwang S, et al. Dysregulated expression of proteins associated with ER stress, autophagy and apoptosis in tissues from nonalcoholic fatty liver disease. *Oncotarget.* 2017;8(38):63370–63381. doi:10.18632/oncotarget.18812
47. Toriguchi K, Hatano E, Tanabe K, et al. Attenuation of steatohepatitis, fibrosis, and carcinogenesis in mice fed a methionine-choline deficient diet by CCAAT/enhancer-binding protein homologous protein deficiency. *J Gastroenterol Hepatol.* 2014;29(5):1109–1118. PMID: 24329600. doi:10.1111/jgh.12481
48. Wong SK, Chin KY, Ahmad F, Ima-Nirwana S. Biochemical and histopathological assessment of liver in a rat model of metabolic syndrome induced by high-carbohydrate high-fat diet. *J Food Biochem.* 2020;44(10):e13371. doi:10.1111/jfbc.13371
49. Sampath C, Rashid MR, Sang S, Ahmedna M. Specific bioactive compounds in ginger and apple alleviate hyperglycemia in mice with high fat diet-induced obesity via Nrf2 mediated pathway. *Food Chem.* 2017;226:79–88. doi:10.1016/j.foodchem.2017.01.056